PHYSICAL REVIEW C VOLUME 19, NUMBER 1 JANUARY 1979

Cross-section and polarization measurements of p-^{4}He elastic scattering at GeV energies

H. Courant, K. Einsweiler, T. Joyce, H. Kagan, Y. I. Makdisi, M. L. Marshak, B. Mossberg, E. A. Peterson, K. Ruddick, and T. Walsh
School of Physics, University of Minnesota, Minneapolis, Minnesota 55455

G. J. Igo, R. Talaga, and A. Wriekat
Physics Department, University of California, Los Angeles, California 90024

R. Klem
Accelerator Research Facilities Division, Argonne National Laboratory, Argonne, Illinois 60439
(Received 23 December 1977)

We have measured the differential cross-section and the analyzing power (polarization) for p-^{4}He elastic scattering at incident kinetic energies of 0.56, 0.80, 1.03, 1.24, and 1.73 GeV. The experiment used a polarized proton beam incident on a liquid helium target and a single arm magnetic spectrometer to detect elastic scattering. Both the differential cross sections and the analyzing power show structure near $-t = 0.25$ $(\mathrm{GeV}/c)^2$ which decreases in magnitude with increasing energy. Both multiple scattering and optical model interpretations of the data are discussed.

[NUCLEAR REACTIONS elastic scattering, p-^{4}He; GeV energies; measured differential cross section; measured polarization; comparison with theory.]

I. INTRODUCTION

The elastic scattering of protons from helium nuclei at GeV energies has received much theoretical and experimental attention in recent years. In principle, data on this process can be used both to extract parameters of the nucleon-nucleon scattering amplitudes and to obtain information about correlations in the helium nucleus. Such an analysis, however, requires a reliable theoretical model and a number of such models, mostly of the Glauber multiple scattering or optical potential type, have been proposed. Testing of the validity of these models and extraction of the interesting parameters have been hampered because, until now, only differential cross-section data have been available in the GeV energy range, and even those data have been somewhat uncertain.

The first measurements of p-^{4}He elastic scattering in this energy region were done at the Brookhaven Cosmotron about 10 years ago.[1] That experiment reported a deep diffraction minimum near $-t = 0.25$ $(\mathrm{GeV}/c)^2$, where t is the four-momentum transfer squared, which stimulated a number of theoretical efforts to fit the data.[2] In 1974, an experiment using SPES I at Saturne, Saclay, reported new differential cross-section data[3] at about the same incident energy and these data showed only a shallow dip. Because there was no internal normalization, these data were normalized using a laboratory cross-section of 75 mb/sr at $\theta_{\mathrm{lab}} = 10°$. (In the literature, these data are sometimes referred to as Saclay A.) This normalization gave reasonable agreement with the Brookhaven data at small t, but in the region of the secondary maximum, the Saclay and Brookhaven data differed by a factor of 2. Recently, a normalized version of the Saclay data has appeared in the literature[4] (Saclay B.) In addition to the absolute normalization, these data seem to differ from the earlier set by a small change in the laboratory scattering angle and a modification of the small-angle points. These new data are in reasonable agreement with the Brookhaven results, except for the deep dip reported in the earlier experiments.

In the last two years, two independent experiments have attempted to obtain definitive results on p-^{4}He elastic scattering. The experiment reported here used the polarized proton beam of the Argonne zero gradient synchrotron (ZGS) incident on a liquid helium target.[5] Elastic scattering was detected by a single-arm magnetic spectrometer. Although this experiment was designed to measure beam analyzing powers (which are equivalent in the case of this reaction to the polarizing powers or polarizations), differential cross-section data were accumulated simultaneously. The other experiment, at the Berkeley Bevatron,[6] used an α beam incident on a liquid hydrogen target and a double-arm spectrometer. As discussed in Sec. III, the results of these two independent experiments with different systematic uncertainties are consistent within the quoted erros. However, a third experiment, done at the Leningrad cyclotron[7] at an incident energy of 1 GeV, yields cross sec-

tions close to the Saclay B values. In Sec. IV, we place additional constraints on theoretical models with data on spin effects in the scattering process. These latest data have spurred new theoretical efforts to understand p-^{4}He elastic scattering. A summary of these new results comprises Sec. V.

II. EXPERIMENTAL METHOD

This experiment used a polarized proton beam incident on a liquid helium target. Elastic scattering was detected by a 30 m long, two-stage magnetic spectrometer, which is shown in plan view in Fig. 1. The recoil helium nucleus was not detected but the forward proton kinematics insured that the helium nucleus remained in the ground state. This method had the advantages of experimental simplicity and the ability to detect scattering at small t; its disadvantages compared to a double-arm spectrometer were increased background and target empty contributions and poorer center-of-mass frame angular resolution.

The spin-dependent quantity measured in this experiment was the beam analyzing power, namely, the left-right scattering asymmetry for a polarized beam on an unpolarized target. For nucleon-nucleus elastic scattering, the analyzing power must equal the target polarizing power (often called the polarization), which is the spin alignment of the product of the scattering of two unpolarized particles. The direction of the normal to the scattering plane is defined in the conventional manner, so that the analyzing power data presented here are positive when more protons are scattered to the left, looking downstream, for incident proton spin up.

The details of the apparatus and estimates of the experimental uncertainties are discussed in the following sections.

A. Proton beam and monitoring

The incident protons were initially polarized in an ANAC ground-state ion source[8] and accelerated by an electrostatic pre-accelerator and an rf linear accelerator to a kinetic energy of 50 MeV. From the linac, the protons were injected into the ZGS main ring and accelerated to the required energy. The protons were then resonantly extracted and transported to the experiment through an evacuated beam line with a few air gaps. The beam intensity was typically 5×10^8 protons per 500 msec spill; the beam duty cycle was 20%. The spot size on the target was nominally 2 cm vertical by 2 cm horizontal full width at half maximum (FWHM) with a larger spot at the lower energies and a smaller spot at the higher energies. The beam was polarized vertically, normal to the scattering plane, and had a polarization of 70 to 75%. The direction of the proton spin was reversed after every accelerator pulse, in order to average over systematic drifts.

The direction, position, and size of the incident beam were monitored by three x-y proportional chambers read out in an integrated mode. Two chambers were placed upstream of magnet X5B1 and one was attached to the upstream end of the helium target vacuum vessel. The chambers had a wire spacing of 2 mm and the three position measurements fixed the beam trajectory independently of the bend angle in X5B1. During the course of the experiment, the beam varied in angle by less than 1 mrad but the horizontal position moved as much as ±1.5 cm, with a typical period of many hours. (See Fig. 2.) This position change caused the scattering angle to vary by up to ±20 mrad from nominal. The data from the proportional chambers were used to correct the nominal scattering angle, but we estimate an uncertainty of ±3 mrad in the absolute scattering angle due to these beam fluctuations.

The intensity of the incident beam was monitored separately for proton spin up and down by a single three-scintillation-counter telescope located in the vertical plane. The telescope had 2.5 cm by 7.5 cm by 1.3 cm scintillators attached directly to RCA 8575 photomultiplier tubes; the largest dimension of the scintillators was in the horizontal plane, perpendicular to the beam axis. This

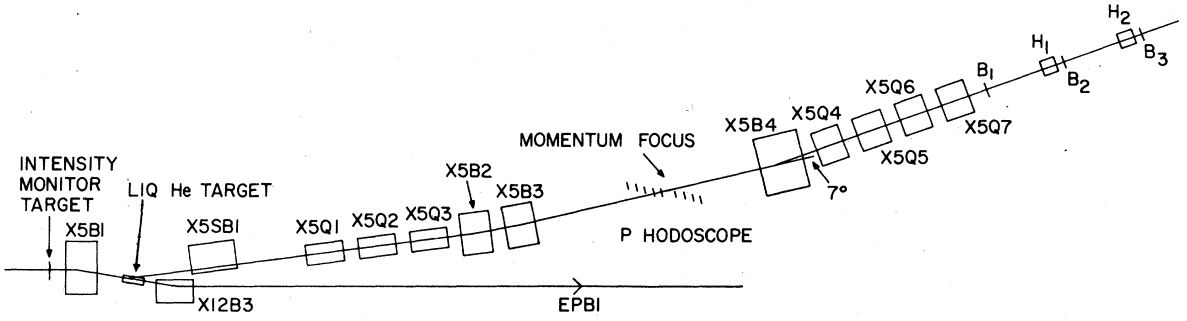

FIG. 1. A schematic view of the experimental apparatus.

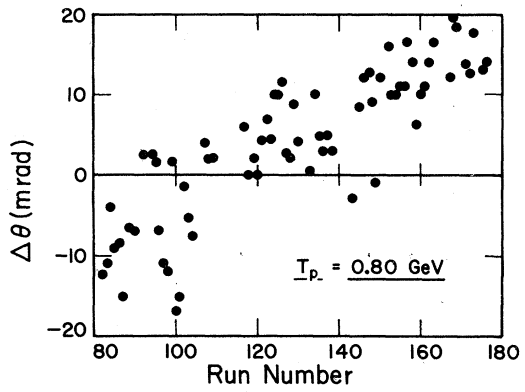

FIG. 2. The deviation of the incident beam from its nominal axis as a function of data collection run number. The period represented by the entire graph was 109 hours.

telescope accepted particles scattered from a thin polyethylene target, much larger in dimension than the beam, which was located about 5 m upstream of the liquid helium target. Since the cross sections at each incident energy of this experiment were normalized without regard to the relative monitors (see Sec. III A), it was only necessary that the calibration of the intensity monitor not change during the four or five days required to accumulate data at one incident energy. The main check on the monitor calibration was that, in general, adjacent kinematic points were measured at different times. The smoothness of the cross section, that is, the extent to which each point lay on the interpolated curve between neighboring points, indicated that monitor calibration drifts did not occur at the 5% level. As a secondary test, the relative intensity monitor was compared with an ion chamber placed in the beam between the polyethylene and helium targets. This chamber provided only a gross check, since its calibration had fluctuations at the 10% level. These tests and ancillary checks on photomultiplier tube characteristics showed no measurable changes in the relative intensity monitor during the experiment. There was also no evidence for spin-dependent fluctuations in the intensity monitor calibration.

The polarization of the incident protons was measured by a carbon target elastic scattering polarimeter located at the end of the 50 MeV linac. The polarimeter had an absolute analyzing power of 0.87 ± 0.03.[9] Previous experiments[10] have shown that there are no depolarizing resonances and no measurable depolarization in the ZGS for proton momenta below 3 GeV/c. We ascribe a normalization error of ±4% to the analyzing powers reported here as a result of both the uncertainty in the polarimeter analyzing power and the possible depolarization of the protons in the synchrotron.

B. Helium target

The helium target flask was a 5 cm diameter by 10 cm long Kapton cylinder mounted in an evacuated jacket. The target was operated at atmospheric pressure. The liquid level was maintained by replenishment from an 18 liter reservoir, which was surrounded by a liquid nitrogen jacket to reduce helium losses. For target empty runs, the liquid helium was forced out of the target flask and replaced by helium gas at temperatures near the boiling point.

From the nominal target helium consumption of 1 liter per hour, it was possible to determine that, on average, less than 2% of the flask volume could be filled with gas rather than liquid. This amounts to a negligible normalization error. The possibility that random, rapid boiling occurred was checked by examining the cross-section ratio for target liquid to target empty (gas) and by noting the smoothness of the ratio (see Fig. 3) and the cross section for neighboring kinematic points measured at different times. No singular effects were found at the 5% level. The target pressure monitors also indicated that rapid boiling did not occur during the data collection portion of the experiment. Data such as those in Fig. 3 also indicated that density fluctuations of the empty target gas occurred at a level of less than 1% of the full target density.

C. Spectrometer

The spectrometer used in this experiment was actually designed as a high-intensity, secondary beam line with good momentum resolution. In the first stage, four dipole magnets provided momentum dispersion and bent the spectrometer axis away from the primary beam line; three quadrupole magnets created a spatial focus about 15 m downstream of the target. The second stage used a 2 m dipole with a 7° bend and two pairs of quadrupoles with equal gradients in each member of the pair to form a second focus. The design production angles were 0° for negatives and 3° for

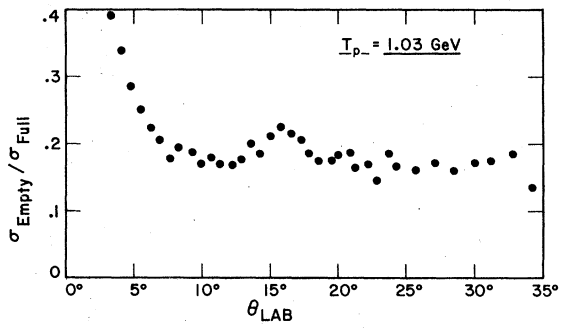

FIG. 3. The ratio of target empty (gas) to target full cross sections for $T_p = 1.03$ GeV. The local maximum in the ratio near $\theta_{lab} = 16°$ corresponds to the diffraction minimum in the differential cross section.

positives.

In order to achieve the large laboratory scattering angles required in this experiment, a number of modifications were made to the upstream end of the spectrometer. The incident beam was bent by dipole magnet X5B1 by as much as 28° from its nominal axis to increase the angle between the incident beam and the spectrometer. The liquid helium target was moved under remote control to intercept the beam in its new position. Septum magnet X12B3 was also movable and was used to begin restoration of the proton beam to its nominal axis for transport to an experiment downstream. The scattered protons were bent to the spectrometer axis by septum magnet X5SB1, which was also remotely movable. At the smallest laboratory scattering angle (about 3.5°), dipole magnet X5B1 was turned off, the helium target was on the nominal proton beam line, and dipole magnet X5SB1 was bending proton trajectories to the left, looking downstream. At the largest angles, X5B1 and X5SB1 were both bending to the right and the target was far to the right of the nominal beam line, all directions looking downstream. For a scattering angle of 14.5°, X5SB1 was turned off and X5B1 bent protons to the right.

Protons in the spectrometer were detected by an x hodoscope (P) at the first focus and by two x and one y hodoscopes (H1 and H2) near the second focus. The P hodoscope consisted of 10 scintillation counters arranged to form 19 overlapping bins, with each bin having a width of 1.3 mm. The outer bins were defined by only one counter, while the central bins were defined by a coincidence of as many as five counters. The first focus of the spectrometer was at the center of the hodoscope, but the outer counters were as much as 25 cm upstream or downstream of the focus. The second spectrometer focus was at hodoscope H1, which consisted of 9 scintillation counters overlapped to form 2.5 mm bins. (For the $T_p = 1.24$ GeV data collection run, H1 was composed of 8 scintillation counters, overlapped to form 5.1 mm bins.) The H2 hodoscope, which was 2 m downstream of H1, had $8x$ and $6y$ scintillation counters; both the horizontal and vertical overlap bins had a width of 5.1 mm. The H1 and H2 hodoscopes each occupied 25 cm along the beam line. The other elements of the spectrometer were an adjustable collimator just downstream of X5SB1 and two scintillation counters B1 and B2 at the end of the spectrometer which were used for triggering. The entire length of the spectrometer was evacuated, except for small regions at the upstream end and around the scintillation counters.

Because of the large apparent target size, the second stage of the spectrometer alone was used to analyze the momentum of the scattered particles. The field in the dipole magnet in this stage was monitored by nuclear magnetic resonance techniques (NMR). The hodoscope data were used to determine the intercept of the particle trajectory with the first and second focal planes of the spectrometer; using those intercepts and the magnetic properties of the spectrometer, the particle momenta were determined. All of the events collected with a single setting of the spectrometer were considered as one angular bin. The spectrometer parameters were fixed empirically by fitting elastic peaks at small angles, where the backgrounds were negligible. This procedure was followed at each incident momentum and the results were in good agreement with the calculated values. The spectrometer momentum acceptance was also determined empirically, by noting the displacement of the elastic peak for a small change in the currents of all the spectrometer magnets. The principal properties of the spectrometer are noted in Table I.

D. Data collection and analysis

The data for this experiment were collected during August and September, 1976. Each incident energy required 4 or 5 days of data-taking time and the incident energies were done in the order 1.24, 0.80, 0.56, 1.73, and then 1.03 GeV. Within each energy, the different angular points were measured in a somewhat random order; in general, adjacent kinematic points were measured at different times. The hodoscope data were written event by event on magnetic tape by a PDP-9 computer, which analyzed a fraction of the data on line. Other information, such as a beam polarization and position and beam intensity monitor data, were summarized on scalers and recorded

TABLE I. Principal properties of the spectrometer.

Length	30 m
Magnets	5 dipoles, 7 quadrupoles
Acceptance	4×10^{-4} sr (laboratory)
Angular resolution	< 12 mrad FWHM
Momentum resolution ($\Delta p/p$)	Typically 0.7% FWHM at T_p = 1.03 GeV (larger at lower energies; smaller at higher energies)

manually and by photograph at the end of each run. Important quantities were double scaled. The data at most of the kinematic points were accumulated in one target full and one target empty data run; on occasion, extra runs were done as checks.

The final data analysis was done completely off line, using the magnetic tapes recorded during the experiment. The software for the CYBER 74 computer used for data analysis was modified from a set of programs used for over two years to analyze data from this spectrometer. In the analysis process, the scattered proton momentum was reconstructed for each event and histograms were accumulated separately for events with incident proton spin up and down. Then, appropriately normalized target empty (gas) momentum spectra were subtracted from the target full spectra. The target empty rate under the elastic peak varied from 30% of the target full rate at small scattering angles to 15% at the larger angles. A target empty rate of about 10% was expected from the residual gas in the target; the remaining target empty effect was presumably from interactions in the flask walls, vacuum windows, and other material in the incident beam.

Examples of the target full and the target empty spectra are shown in Fig. 4 for a point in the region of the cross-section dip at $T_p = 1.03$ GeV. This point has the worst signal-to-background ratio at this energy. The data at the cross-section dip at higher incident energies have larger backgrounds (33 percent of the elastic peak at 1.24 GeV and 20 percent at 1.73 GeV); at lower incident energies, the background is smaller. The data at 1.24 GeV were taken before the H1 hodoscope was modified to improve the spectrometer resolution (see Sec. II C) and, consequently, had the worst signal-to-background ratio. For the cross-section analysis, the signal was isolated from the background by assuming a Gaussian shape for the elastic peak. The high momentum side of the peak (right-hand side in Fig. 4) was assumed free of background in the fitting process. The validity of these assumptions was confirmed by the small angle data where the background was negligible and the entire elastic peak could be uniquely resolved. An error of ±20% of the subtracted background which occurred between $\pm\sigma$ of the center of the elastic peak has been added in quadrature to account for the uncertainties in the background subtraction process. This uncertainty was estimated from the variability of the results obtained from various methods of fitting the elastic peak and the background.

For the analyzing power measurements, it was possible to reduce the backgrounds before the subtraction by making a cut on the data for the scattered proton position at the first focus. Such a cut has no effect on the analyzing power measurement, other than to reduce the number of events, if it is made impartially for the events with incident proton spin up and down. Figure 4(b) was obtained from Fig. 4(a) by removing all events with a proton horizontal position >+5 mm (+ is downstream left) from the spectrometer axis at the first focus. The effects of this cut suggest that

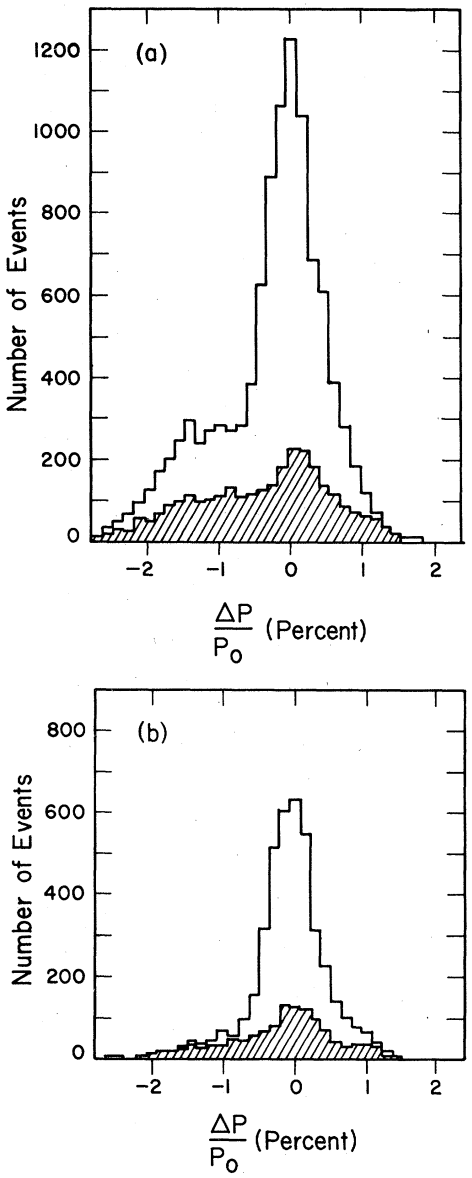

FIG. 4. Reconstructed forward proton momentum spectra for $T_p = 1.03$ GeV in the region of the first diffraction minimum. The shaded spectra are for target empty (gas) events. The upper graph is typical of histograms used for the cross section determination; histograms similar to the lower diagram were used to determine the analyzing power (see text).

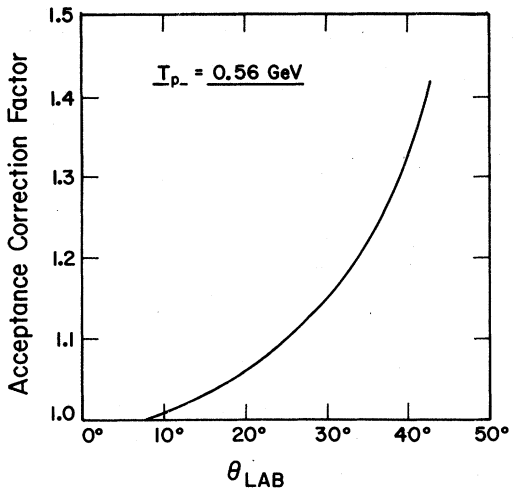

FIG. 5. The acceptance correction used for the differential cross-section data at $T_p = 0.56$ GeV. Corrections used for other incident momenta were similar at similar lab angles.

some of the background may have come from low momentum particles scattered from the 2.5 cm septum of X5SB1. This cut removed enough of the background so that the systematic error in the analyzing power due to background was negligible.

At laboratory scattering angles larger than 20°, the acceptance of the spectrometer was reduced by limiting apertures which prevented transport of particles scattered from the ends of the target. The magnitude of this effect, which ranged up to 40%, was calculated using the Monte Carlo program TURTLE.[11] The calculated correction, shown in Fig. 5, was applied to the cross-section data and an error of ±20% of the correction was added in quadrature. This correction had no effect on the analyzing power data.

III. CROSS-SECTION DATA

A. Normalization and errors

The absolute normalization of the cross-section data at 0.80 and 1.73 GeV was accomplished by substituting for the liquid helium target a 10 cm liquid hydrogen target and measuring pp elastic scattering. Because the hydrogen target was unable to traverse across the incident beam, this measurement could be made at only one scattering angle for each of these incident energies. Given the pp elastic cross section from a fit to the available data,[12] it was possible to determine the absolute p-^{4}He elastic cross sections at these same incident energies and scattering angles by the equation

$$\frac{d\sigma'}{d\Omega'} = \frac{d\sigma}{d\Omega}\frac{N'}{N}\frac{J}{J'}\frac{\rho}{\rho'}\frac{l}{l'}\frac{1}{S},$$

where the primed quantities refer to the p-^{4}He scattering and the unprimed quantities refer to pp scattering. In this equation, $d\sigma/d\Omega$ is the center-of-mass cross section, N is the number of events normalized to the relative intensity monitor, J is the Jacobian for the transformation of the solid angle from the laboratory to the center-of-mass frame, ρ is the density of the target liquid, l is the target length (in this case, $l = l'$), and S is a correction factor for the spectrometer acceptance, because the helium and hydrogen targets were different distances from the spectrometer quadrupoles. The parameters used for this normalization are listed in Table II. S was determined by Monte Carlo calculation. Since it has a value near unity, the uncertainty in this factor made a negligible contribution to the overall normalization error. This normalization procedure eliminated most of the uncertainties in the determination of the spectrometer acceptance and eliminated the necessity for an absolute calibration of the relative intensity monitor.

The cross-section data at these two energies, 0.80 and 1.73 GeV, were then fit to the form $d\sigma/dt = A \exp Bt$, for $|t| < 0.1$ (GeV/c)^2, as shown in Fig. 6. These differential cross-section fits were integrated ($\int d\sigma/dt = A/B$) to yield a total p-^{4}He elastic cross-section of 31.5 mb at each of these two incident energies. The data at the other three energies (0.56, 1.03, and 1.73 GeV) were normalized by the same fitting and integration procedure combined with the *assumption* that the total elastic cross section at these energies was also 31.5 mb.[13]

TABLE II. Parameters used in the normalization procedure.

Incident energy (GeV)	0.80	1.73
t (GeV/c)^2	1.29×10^{-2}	2.62×10^{-2}
pp cross-section fit [$d\sigma/dt$ (mb/(GeV/c)^2)]	130 exp6t	115 exp7.5t
pp cross-section [$d\sigma/dt$ (mb/(GeV/c)^2)] at t used for normalization	120	92
Hydrogen density [ρ (g/cm^3)]	0.071	0.071
Helium density [ρ' (g/cm^3)]	0.125	0.125
Acceptance correction (S)	1.2	1.2

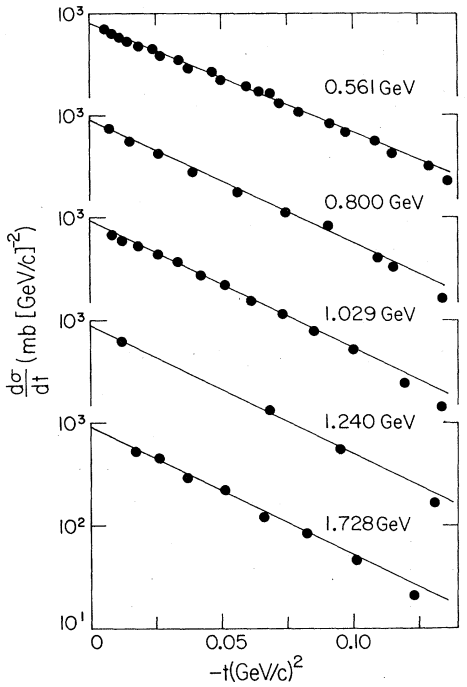

FIG. 6. Fits to the differential cross section of the form $d\sigma/dt = A \exp Bt$ for $t < 0.1$ (GeV/c)^2. The numerical coefficients determined from the fit are listed in Table V.

We estimate the error in this normalization procedure as ±15%. This uncertainty arises from the imprecise knowledge of the pp cross section and possible systematic errors in the normalization procedure. This quantity should be construed as both a possible overall normalization shift and a possible energy dependence in the total elastic cross section.

Sufficient elastic events and monitor counts were recorded at each kinematic point so that the statistical errors in all of the cross sections were negligible compared to the systematic errors. The point-to-point systematic error was determined by the following procedure: An uncertainty of ±5% based on the smoothness and repeatibility of the data was assigned to each cross-section measurement. Factors for the uncertainties mentioned above were then added in quadrature. The resultant systematic error for each cross-section point is listed with the data in Table IV.

Because of the complex arrangement of the upstream end of the spectrometer, the absolute value of t was best determined by the measurement of the absolute momentum differences between the incident and scattered protons and the use of elastic scattering constraints. The spectrometer momentum determination was calibrated against the incident momentum at small angles where the difference was small; the dipole magnet which determined the scattered momentum was monitored by NMR techniques as the scattering angle was changed. We estimated the uncertainty in the absolute momentum determination of the central spectrometer trajectory (not the uncertainty in the momentum of any particular scattered particle) as ±0.5%. From the p-^{4}He elastic kinematics, it was possible to determine the absolute t uncertainties listed in Table III.

B. Differential cross section

The p-^{4}He elastic differential cross-section data measured in this experiment are shown in Fig. 7 and listed in Table IV. The data at all energies show the usual structure of a diffraction dip followed by a secondary maximum. The dip is centered at $-t = 0.28$ (GeV/c)^2 at $T_p = 0.56$ GeV and moves to slightly larger momentum transfer as the incident energy increases. At the highest incident energy $T_p = 1.73$ GeV, there is a change of slope in the region near $-t = 0.8$ (GeV/c)^2, which is where double and triple scattering amplitudes are of comparable magnitude.

The comparison of these results with previous and contemporaneous measurements is shown in Figs. 8 and 9. Figure 8 compares our cross section measurements at 0.56 GeV with data from several previous experiments[14] at incident kinetic energies between 0.50 and 0.65 GeV. The data agree well in shape and the difference in the absolute normalizations is within the ±15% normalization error in this experiment without regard to the normalization errors in the other data sets. The data at an incident kinetic energy near 1 GeV are considerably more perplexing, as indicated in Fig. 9. Including the data reported here, there

TABLE III. Absolute uncertainties in t as a function of incident kinetic energy.

Kinetic energy (GeV)	Uncertainty in t (GeV/c)^2
0.56	±0.01
0.80	±0.02
1.03	±0.02
1.24	±0.03
1.73	±0.03

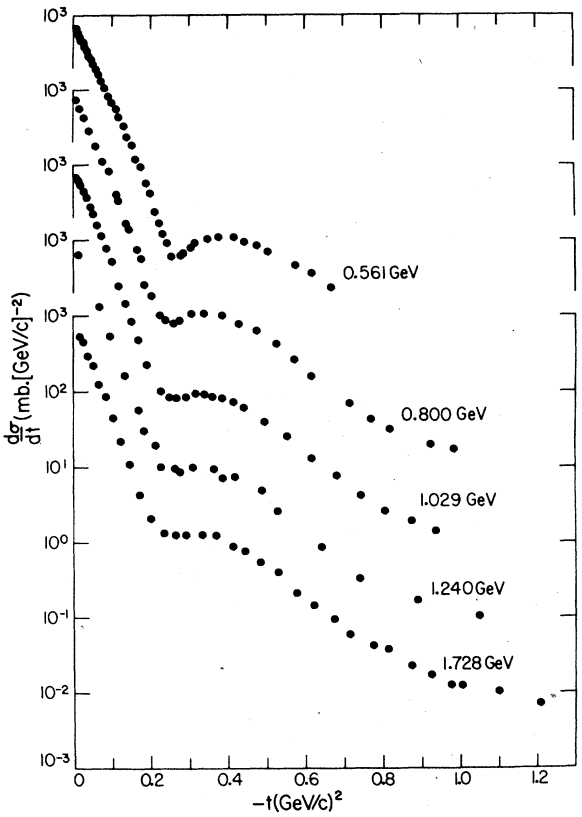

FIG. 7. The differential cross-section for p-^{4}He elastic scattering as a function of t, the four-momentum transfer squared.

have been four recent experiments studying p-^{4}He elastic scattering in this energy region. There is general agreement on the shape of the differential cross section, including the observation of only a shallow dip in contrast to the observations in Ref. 1. Each of the four experiments was internally normalized with quoted normalization uncertainties of approximately ±15%. The absolute cross sections, however, cluster in two distinct regions. The cross-sections reported by Aslanides *et al.*[4] and Alkhazov *et al.*[7] are approximately a factor of 2 larger than the cross sections found in this experiment and by Geaga *et al.*[6] The experiments in each group agree well within the specified uncertainties, but there is no apparent explanation for the discrepancy between the two sets of experiments. It should be noted that the procedures used by Geaga *et al.* and this experiment were very different. The Berkeley experiment used an α beam, a gas target, a double-arm spectrometer and a direct, beam-counting normalization method. This experiment used a proton beam, a liquid target, a single-arm spectrometer, and a ratio-to-pp normalization method. Many of these elements were also present in the experiments reported in Refs. 4 and 6.

Theoretical calculations, both of the multiple scattering and the optical potential type, indicate that the structure of the cross section in the region of the dip is sensitive to the detailed characteristics of the model. It is useful, therefore,

TABLE IV. The p-^{4}He elastic scattering cross sections and analyzing powers measured in this experiment.

$-t$ (GeV/c)^2	$d\sigma/dt$ mb/(GeV/c)^2	Error in $d\sigma/dt$ (± %)	Polarization	Error (±)
T_p = 0.56 GeV				
0.0057	690	5	0.242	0.030
0.0081	622	5	0.306	0.015
0.0108	587	5	0.364	0.012
0.0140	536	5	0.394	0.015
0.0186	484	5	0.399	0.010
0.0240	450	5	0.391	0.013
0.0265	382	5	0.417	0.010
0.0336	347	5	0.469	0.011
0.0374	293	5	0.489	0.009
0.0464	268	5	0.501	0.009
0.0500	227	5	0.488	0.009
0.0593	193	5	0.492	0.009
0.0643	166	5	0.461	0.010
0.0716	133	5	0.415	0.009
0.0793	107	5	0.366	0.011
0.0909	84.0	5	0.384	0.012
0.0970	69.0	5	0.344	0.009
0.108	56.2	5	0.326	0.013
0.115	42.5	5	0.275	0.011
0.129	32.0	5	0.260	0.009

TABLE IV. *(Continued)*

$-t$ (GeV/c)^2	$d\sigma/dt$ mb/(GeV/c)^2	Error in $d\sigma/dt$ (± %)	Polarization	Error (±)
0.136	23.5	5	0.223	0.014
0.151	18.7	5	0.194	0.011
0.158	11.7	5	0.112	0.017
0.173	9.26	5	0.090	0.016
0.186	5.75	5	−0.012	0.020
0.197	4.22	5	−0.098	0.020
0.208	2.43	5	−0.189	0.024
0.222	1.73	5	−0.287	0.020
0.229	1.21	6	−0.392	0.032
0.242	0.905	6	−0.348	0.026
0.254	0.600	6	−0.189	0.045
0.277	0.617	6	−0.023	0.030
0.283	0.682	6	0.173	0.027
0.305	0.797	6	0.366	0.021
0.313	0.939	6	0.484	0.022
0.345	1.05	6	0.576	0.023
0.378	1.11	7	0.524	0.019
0.414	1.10	7	0.456	0.022
0.440	0.948	7	0.434	0.022
0.473	0.849	7	0.373	0.018
0.502	0.707	8	0.394	0.021
0.573	0.480	9	0.360	0.026
0.612	0.375	10	0.337	0.025
0.662	0.235	11	0.231	0.037
T_p = 0.80 GeV				
0.0071	743	5	0.189	0.010
0.0150	574	5	0.268	0.009
0.026	421	5	0.313	0.009
0.039	285	5	0.352	0.009
0.056	177	5	0.370	0.007
0.074	111	5	0.372	0.008
0.091	81.7	5	0.373	0.009
0.109	40.1	5	0.326	0.009
0.115	33.1	5	0.323	0.009
0.134	16.9	5	0.294	0.012
0.142	14.0	5	0.269	0.011
0.161	7.32	5	0.198	0.010
0.171	5.74	5	0.163	0.009
0.181	2.53	5	0.066	0.013
0.203	1.83	5	0.011	0.018
0.223	1.00	5	0.038	0.016
0.237	0.869	5	0.115	0.022
0.259	0.796	5	0.352	0.015
0.274	0.863	5	0.425	0.012
0.305	1.06	5	0.492	0.012
0.337	1.07	5	0.491	0.011
0.385	0.992	5	0.504	0.012
0.427	0.796	5	0.465	0.013
0.473	0.623	5	0.412	0.014
0.522	0.421	5	0.413	0.014
0.569	0.265	6	0.392	0.018
0.613	0.160	6	0.359	0.032
0.713	0.0694	7	0.262	0.035
0.769	0.0436	7	0.232	0.075
0.818	0.0316	8	0.165	0.046

TABLE IV. *(Continued)*

$-t$ (GeV/c)^2	$d\sigma/dt$ mb/(GeV/c)^2	Error in $d\sigma/dt$ (± %)	Polarization	Error (±)
0.923	0.0199	9	0.261	0.049
0.983	0.0174	10	0.207	0.064
T_p = 1.03 GeV				
0.0082	692	5	0.140	0.013
0.012	612	5	0.145	0.015
0.018	525	5	0.191	0.011
0.026	439	5	0.206	0.011
0.033	372	5	0.225	0.010
0.042	272	5	0.214	0.011
0.051	225	5	0.240	0.011
0.061	155	5	0.241	0.010
0.073	115	5	0.238	0.011
0.085	78.4	5	0.241	0.011
0.099	51.9	5	0.248	0.011
0.119	24.7	5	-	-
0.134	14.6	5	0.228	0.017
0.149	8.46	5	0.248	0.015
0.168	4.85	5	0.219	0.017
0.190	2.31	5	0.121	0.015
0.227	1.01	5	0.155	0.014
0.247	0.839	5	0.237	0.014
0.267	0.806	5	0.342	0.015
0.292	0.819	5	0.362	0.016
0.314	0.946	5	0.391	0.013
0.337	0.902	5	0.421	0.014
0.360	0.850	5	0.442	0.014
0.384	0.806	5	0.429	0.013
0.413	0.719	5	0.397	0.013
0.438	0.601	5	0.426	0.013
0.492	0.392	5	0.325	0.015
0.551	0.252	5	0.330	0.020
0.164	0.130	5	0.337	0.023
0.679	0.0775	5	0.345	0.027
0.742	0.0423	6	0.282	0.035
0.806	0.0260	6	0.324	0.037
0.873	0.0187	6	0.304	0.046
0.936	0.0138	7	0.262	0.033
T_p = 1.24 GeV				
0.012	640	5	0.129	0.017
0.068	131	5	0.224	0.013
0.095	54.4	5	0.261	0.010
0.131	16.7	5	0.272	0.023
0.170	5.66	5	0.174	0.023
0.181	3.01	9	0.182	0.019
0.213	1.96	6	0.153	0.015
0.226	0.998	9	0.191	0.018
0.262	0.954	5	0.265	0.012
0.276	0.854	5	0.320	0.020
0.308	0.981	5	0.376	0.015
0.364	0.932	5	0.395	0.009
0.384	0.700	5	0.405	0.015
0.417	0.733	5	0.378	0.014
0.486	0.483	6	0.402	0.013
0.527	0.254	5	0.370	0.015

TABLE IV. (*Continued*)

$-t$ (GeV/c)^2	$d\sigma/dt$ mb/(GeV/c)^2	Error in $d\sigma/dt$ (±%)	Polarization	Error (±)
0.643	0.0851	5	0.295	0.029
0.741	0.0332	6	0.200	0.039
0.889	0.0167	8	0.191	0.040
1.05	0.0102	8	0.341	0.077
T_p = 1.73 GeV				
0.017	526	5	0.113	0.010
0.026	424	5	0.124	0.015
0.037	294	5	0.123	0.013
0.051	220	5	0.127	0.018
0.066	122	5	0.165	0.015
0.082	86.3	6	0.185	0.016
0.103	45.9	6	0.195	0.014
0.123	21.4	6	0.212	0.014
0.145	10.8	6	0.161	0.014
0.173	4.22	6	0.134	0.024
0.199	2.06	6	0.116	0.025
0.234	1.31	6	0.187	0.028
0.264	1.24	6	0.211	0.014
0.291	1.26	5	0.287	0.016
0.333	1.25	5	0.313	0.014
0.368	1.26	6	0.278	0.015
0.410	0.843	6	0.315	0.017
0.442	0.778	6	0.309	0.010
0.482	0.536	6	0.286	0.015
0.529	0.401	6	0.262	0.013
0.578	0.211	6	0.282	0.016
0.622	0.143	6	0.248	0.020
0.674	0.0920	6	0.272	0.021
0.715	0.0599	6	0.246	0.022
0.777	0.0439	6	0.219	0.029
0.813	0.0386	6	0.200	0.032
0.872	0.0224	6	0.215	0.039
0.924	0.0172	6	0.254	0.043
0.978	0.0123	6	0.243	0.046
1.03	0.0123	6	0.274	0.044
1.10	0.0105	7	0.314	0.051
1.21	0.00703	8	0.373	0.054

to study the cross sections in the region of the dip and the secondary maximum as a function of incident energy. These data are shown in Fig. 10(a). Unfortunately, the normalization discrepancies among experiments with incident energies near 1 GeV, confuse this graph. In Fig. 10(b), the ratio R of the differential cross-section at the secondary maximum to the differential cross section at the dip is plotted for each experiment. All experiments agree on the sharp structure in R near T_p = 650 MeV, although there is some unexplained discrepancy among experiments on the exact value of the ratio at this point. Above 1 GeV, R reaches a value of almost unity, but a CERN experiment[16] at T_p = 23.1 GeV, (not shown on the graph) yields an R value of 7, indicating that R increases considerably at higher energies. The R at 1.03 GeV of 1.17 ± 0.08 measured in this experiment can be contrasted with the optical model calculations of Lambert and Feshbach and Kujawski,[2] which yield R's ranging from 2.5 to 4.8, depending on the assumptions made about the correlations of the nucleons in the helium nucleus. It should be noted that these calculations attempted to fit the Brookhaven data, which have an anomalously large dip. The multiple scattering calculation of Wallace and Alexander[17] and the optical model fits of Mercer *et al.*[18] yield R values which are consistent with this experiment.

The slopes and intercepts for the small angle fits to the differential cross-sections are listed in Table V. These slopes presumably reflect both the helium form factor and the slopes of the nucleon-nucleon scattering amplitudes. Figure 11

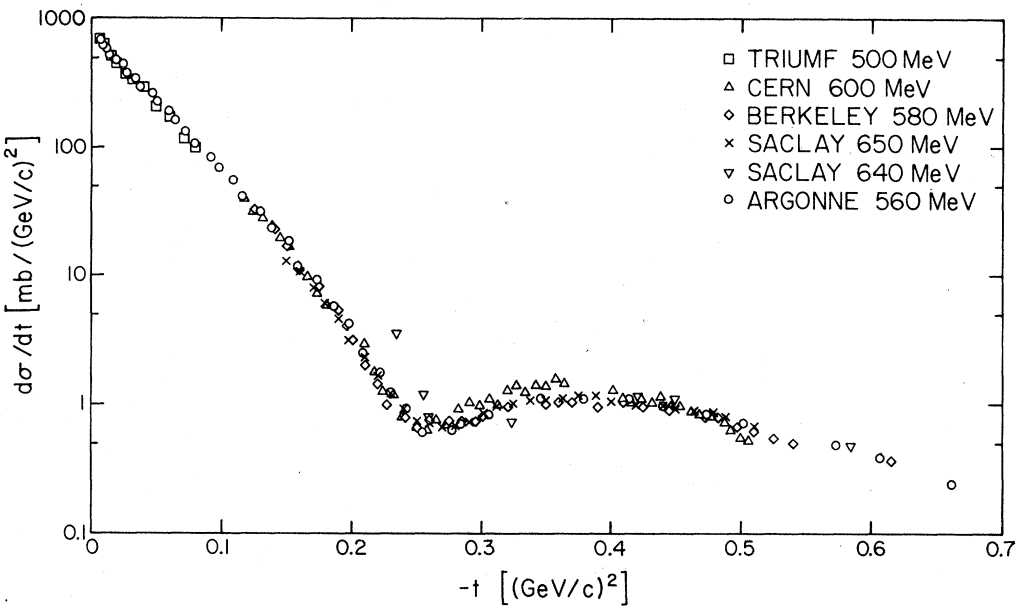

FIG. 8. A comparison of the differential cross-sections measured in this experiment at $T_p = 0.56$ GeV with previous data in this incident energy region. The data shown are from Ref. 14.

shows the p-^{4}He cross-section slopes and the NN cross-section slopes as a function of incident energy. The former have been divided by 4 in order to fit all of the data conveniently on the same graph. It is apparent from the graph that both the nucleon-nucleon and nucleon-nucleus slopes change at approximately the same incident energy.

The differential cross section intercepts at $t = 0$ permit an estimate of the total p-^{4}He total cross section through the optical theorem. The quantities $4\pi k(d\sigma/d\Omega)^{1/2}$, which are listed in Table V, are an upper limit to the total cross section. If the ratio of the real to the imaginary part of the p-^{4}He scattering amplitude is similar to the ratio α_{pp} (Ref. 19) which has been measured at these energies, then the contribution of the real part to the forward cross section is small. For this case the p-^{4}He total cross sections are listed in Table V. These quantities should be compared with the measurement of $\sigma_T = 152 \pm 8$ mb at $T_p = 1.0$ GeV measured in the Brookhaven experiment.[1]

IV. ANALYZING POWER DATA

A. Experimental uncertainties

The errors in the analyzing power data were primarily statistical. The alternation of the sign of the incident beam polarization with every accelerator pulse eliminated systematic errors due to long-term drifts. Only effects which were directly correlated with the sign of the incident proton spin could have resulted in an error in the analyzing power. Polarization-dependent effects were observed in the incident beam intensity and polarization, in the target empty rate and in the background subtraction. These factors were all considered in the analysis of the analyzing power data. We found no evidence for a spin dependence in the incident beam position, the spectrometer solid angle or the calibration of the relative intensity monitor. For these reasons, we have not included any systematic effects in the uncertainties listed in Table IV. Because of possible errors in the absolute calibration of the 50 MeV polarimeter[9] and the possibility of depolarization of the protons during acceleration,[10] we have estimated an overall normalization uncertainty of ±4% *of the analyzing power* due to imprecise knowledge of the incident beam polarization.

B. The data

The analyzing power data are shown in Fig. 12 along with previous results at $T_p = 0.54$ GeV.[20] The general features are a rise from the symmetry-required zero in the forward direction to a maximum near $-t = 0.1$ (GeV/c)^2, a dip in the vicinity of $-t = 0.25$ (GeV/c)^2 and then a rise to a second maximum. At the highest incident energies, a second shallow minimum occurs near $-t = 0.8$ (GeV/c)^2. The magnitudes of these features vary with energy, but the second maximum generally has a larger magnitude than the first. The dip in the analyzing power is particularly prominent at $T_p = 0.56$ GeV and it becomes more shallow as the incident energy increases.

The agreement with previous data is good except

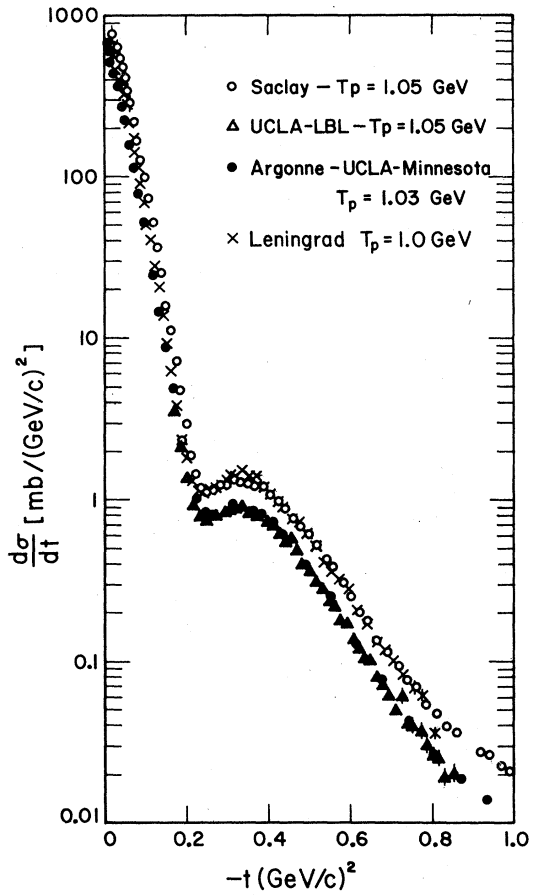

FIG. 9. A comparison of the differential cross-sections measured in this experiment $T_p = 1.03$ GeV with previous results from Saclay (Ref. 4) and recent results from Berkeley (Ref. 6) and Leningrad (Ref. 7).

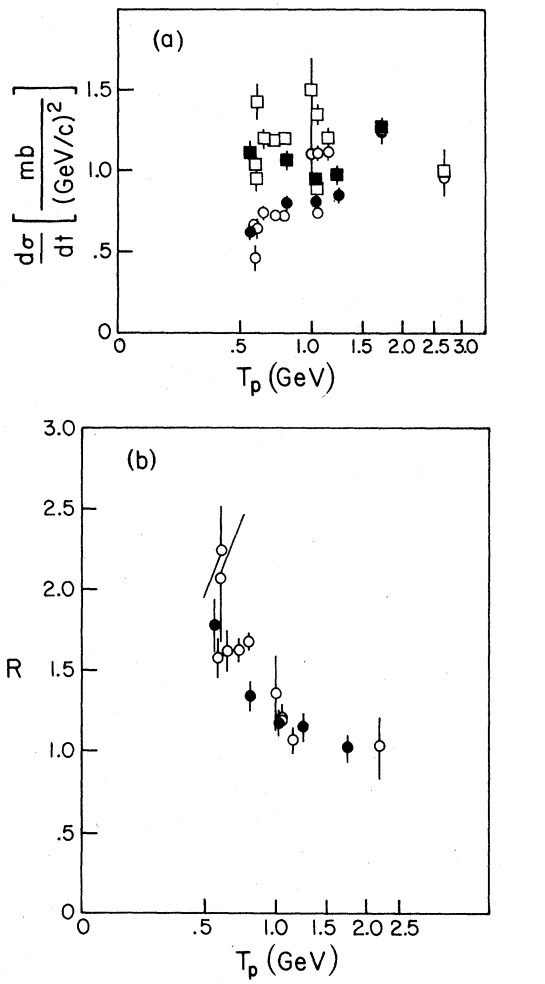

FIG. 10. The differential cross section for p-^{4}He elastic scattering in the neighborhood of the diffractive dip. The upper graph shows the cross section at the dip (○) compared to the cross section at the secondary maximum (□). The lower graph shows the ratio R of these two cross sections. Dark points are from this experiment. Open points are from Refs. 4, 6, 7, 14, and 15.

in the region of the dip at 0.56 GeV. The Space Radiation Effects Laboratory (SREL) data at 0.54 GeV have a shape similar to the present results, but their dip is significantly more shallow. Since the present data set has 5 angular bins in a region where the SREL data have only one bin, it is likely that the disagreement results from the limited angular resolution in the SREL experiment.

TABLE V. Coefficients of small-angle fits of the form $d\sigma/dt = A \exp Bt$ to the elastic differential cross-section and estimates of the total cross-section through the optical theorem. The value of $4\pi k\,(d\sigma/d\Omega)^{1/2} \cong \sigma_T$ is consistent within errors with the measurements of Schwaller *et al.* (Ref. 13).

Incident energy (GeV)	A mb/(GeV/c)	B (GeV/c)$^{-2}$	$4\pi k\,(d\sigma/d\Omega)^{1/2}$ [a] (mb)
0.56	772	24.5 ± 0.1	123
0.80	882	28.0 ± 0.1	131
1.03	898	28.5 ± 0.3	133
1.24	932	29.6 ± 0.8	135
1.73	923	29.3 ± 0.6	134

[a] These numbers have a normalization uncertainty of ± 15 %.

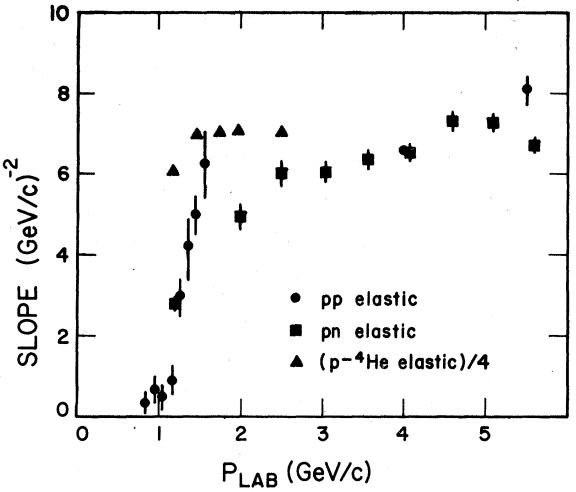

FIG. 11. The slopes of the pp, pn, and p-^{4}He differential cross sections for small t as a function of the incident momentum. The nucleon-nucleus slopes (from this experiment) have been divided by four in order for them to fit conveniently on the same graph.

The gross features of the analyzing power data are easily interpreted in a multiple scattering model. If A is the spin-independent amplitude and C is the spin-flip amplitude, then the analyzing power is proportional to the interference between A and C. However, both A and C have single and double scattering terms, whose imaginary parts are 180° out of phase. The cancellations due to this phase difference cause a dip in the differential cross section in the region where single and double scattering amplitudes are of comparable magnitude. If A and C have a different t dependence, that is, if A_s and A_d (where s and d denote single and double scattering terms, respectively) cancel at different values of t from where C_s and C_d cancel, sharp structure in the polarization will result. The data presented here indicate that either this difference in the t dependence of A and C tends to vanish as the incident energy increases or that the effect of the real part becomes stronger with increasing energy. The same arguments can be used to explain the presence of the dip in the analyzing power near $-t = 0.8$ (GeV/c)^2, in a region where the double and triple scattering amplitudes are of comparable magnitudes. Of course, a detailed model requires a mechanism which will cause a different t dependence for the A and C amplitudes; two examples are discussed in Sec. V.

It is interesting to compare the present analyzing power data with previous predictions based on multiple scattering and optical potential models. As previously mentioned, several of the calculations were based on the Brookhaven data and, as a result, predict incorrect cross sections in the region of the dip. These models also predict nearly saturated ($A \simeq 1$) analyzing powers near the first secondary maximum in the cross section. This feature is also a result of the multiple scattering model of Auger, Gillespie, and Lombard,[21] which more nearly fits the differential cross section. It is clear from the data, which show polarizations no larger than 40% at $T_p = 1.03$ GeV, that all of these calculations have used excessively large magnitudes for the C amplitude in this region. Even at 0.56 GeV, the magnitude of the polarization does not exceed 60%

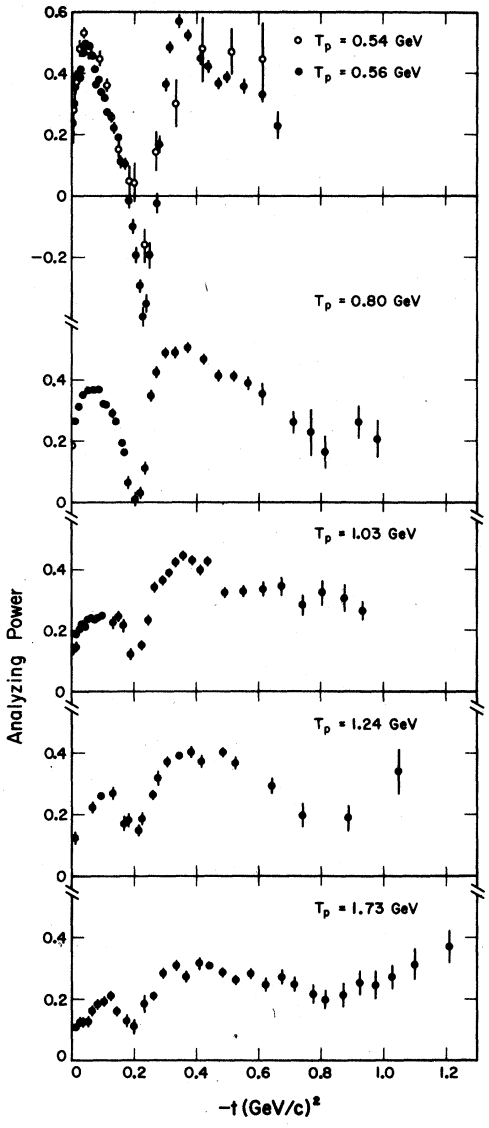

FIG. 12. The analyzing power data measured in this experiment. SREL data at $T_p = 0.54$ GeV from Ref. 20 have been plotted for the purposes of comparison.

V. RECENT INTERPRETATIONS AND CONCLUSIONS

The availability of the present absolutely normalized cross-section data, similar results from Berkeley, and analyzing power measurements have stimulated several theoretical investigations of p-^{4}He elastic scattering. As in the past, both multiple scattering and optical potential model calculations have been pursued with encouraging results in both cases. Wallace and Alexander[17] have fitted the differential cross section and analyzing power at $T_p = 1.03$ GeV. These authors suggest that the inclusion of noneikonal terms in a multiple scattering model should permit a fit to the cross section with an accuracy of better than 5%, but they cannot fit both the cross section and the analyzing power data without the inclusion of an inelastic intermediate state in the multiple scattering formalism. The region $0.2 < -t < 0.4$ $(\mathrm{GeV}/c)^2$ is most sensitive to the $N^*(1232)$ production amplitudes. Inclusion of the intermediate state fills in the cross-section dip and reduces the maximum analyzing power in this region from 0.8 to 0.4, in agreement with the data. The structure in R near $T_p = 650$ MeV is also correlated with the onset of $N^*(1232)$ production. In their model, the fit to the analyzing power data requires $\alpha_{pn} = -0.35$, where α is the ratio of the real to the imaginary part of the scattering amplitude. This quantity can be contrasted with α_{pp}, which is equal to -0.06 at this energy.[19] The differential cross section alone can be well fitted with several arbitrary values for α_{pn}.[22] The analysis of Wallace and Alexander indicates that the study of p-nucleus scattering can yield previously unknown information about the nucleon-nucleon scattering amplitudes.

Mercer, Arnold, and Clark[18] have fitted the cross section and analyzing power at $T_p = 1.03$ GeV using an optical potential model. Theirs is a relativistically correct model which uses a scalar and a fourth-component vector potential. In their model, the ratio of the scalar to the vector potential is particularly sensitive to the spin-orbit potential, which, in turn, is dependent on the analyzing power. Their fit to the measured analyzing power at $T_p = 1.03$ GeV yields a vector to scalar ratio of -0.72, which is consistent with previous calculations based on meson exchange theory. This ratio is insensitive to the differential cross section due to cancellations. Once these authors have fit the $T_p = 1.03$ GeV data, they obtain a reasonable agreement with both the cross section and the analyzing power data at the other incident energies measured in this experiment without any additional parameters.

It is clear to us that recent experiments and the ensuing theoretical investigations of the p-^{4}He system are only a step towards the understanding of proton-nucleus scattering. There are many aspects of the problem which are not well understood. Some cross sections are known but more have not been measured or are in dispute; fewer polarization measurements have been made and the nucleon-nucleon scattering amplitudes, particularly pn, are not well known in the GeV energy region. It is certainly not clear whether either multiple scattering or optical potential models provide a realistic representation of the data. Given this context, it is unlikely in the near future that proton-nucleus scattering will yield quantitative information about correlations within the nucleus. We do, however, plan further measurements in order to clarify the model question and obtain information about the NN amplitudes.[22]

We wish to acknowledge the assistance of the entire staff of the Argonne ZGS, particularly those people responsible for the polarized beam. We are indebted to A. Passi for his design of the spectrometer movement, to Professor L. Price for the loan of equipment, and to G. Bernard and J. Lee for assistance in the data collection phase of the experiment. We thank Professor S. Wallace and Professor B. Clark for providing results from their calculations. This work was supported by the U. S. Department of Energy.

---

[1]H. Palevsky, J. L. Friedes, R. J. Sutter, G. W. Bennett, G. J. Igo, W. D. Simpson, G. C. Phillips, D. M. Corley, N. S. Wall, R. L. Stearns, and B. Gottschalk, Phys. Rev. Lett. 18, 1200 (1967).

[2]Examples of optical model calculations are E. Kujawski, Phys. Rev. C 1, 1651 (1970) and E. Lambert and H. Feshbach, Ann. Phys. (N.Y.) 76, 80 (1973). An example of a multiple scattering calculation is G. I. Lykasov and A. V. Tarasov, Yad. Fiz. 17, 301 (1973) and 20, 489 (1974) [Sov. J. Nucl. Phys. 17, 153 (1973) and 20, 263 (1975)].

[3]S. D. Baker, R. Beurtey, G. Bruge, A. Chaumeaux, J. M. Durand, J. C. Fairre, J. M. Fontaine, D. Garreta, D. Legrand, J. Saudinos, J. Thirion, R. Bertini, F. Brochard, and F. Hibon, Phys. Rev. Lett. 32, 839 (1974).

[4]E. Aslanides, T. Bauer, R. Bertini, R. Beurtey, A. Boudard, F. Brochard, G. Bruge, A. Chaumeaux, H. Catz, J. M. Fontaine, R. Frascaria, D. Garreta, P. Gorodetzky, J. Guyot, F. Hibou, D. Legrand, M. Matoba, Y. Terrien, J. Thirion, and E. Lambert, Phys. Lett. 68B, 221 (1977).

[5]Portions of these data have been reported in R. Klem, G. Igo, R. Talaga, A. Wriekat, H. Courant, K. Einsweiler, T. Joyce, H. Kagan, Y. Makdisi, M. Marshak, B. Mossberg, E. Peterson, K. Ruddick, and T. Walsh,

Phys. Rev. Lett. 38, 1273 (1977); Phys. Lett. 70B, 155 (1977); and in *High Energy Physics With Polarized Beams and Targets*, edited by M. L. Marshak, (AIP, New York, 1976), p. 70.

[6]J. V. Geaga, M. M. Gazzaly, G. J. Igo, J. B. McClelland, M. A. Nasser, A. L. Sagle, H. Spinka, J. B. Carroll, V. Perez-Mendez, and E. T. B. Whipple, Phys. Phys. Rev. Lett. 38, 1265 (1977).

[7]G. D. Alkhazov, A. G. Atamanchuk, S. L. Belostotskii, S. S. Volkov, E. A. Damaskinski, Yu. V. Dotsenko, O. A. Domchenkov, N. P. Kuropatkin, V. N. Nikulin, O. E. Prokof'ev, and M. A. Shuvaev, Zh. Eksp. Teor. Fiz. Pis'ma 26, 110 (1977) [JETP Lett. 26, 1102 (1977)].

[8]Built by Auckland Nuclear Accessories Corporation, Auckland, New Zealand.

[9]E. Parker, private communication.

[10]T. K. Khoe, R. L. Kustom, R. L. Martin, E. F. Parker, C. W. Potts, L. G. Ratner, R. E. Timm, A. D, Krisch, J. B. Roberts, and J. R. O'Fallon in *Proceedings of the Ninth International Conference on High Energy Accelerators,1974,* CONF-740522 (National Technical Information Service, Springfield, Virginia).

[11]D. C. Carey, Report No. NAL-64, 1971 (unpublished).

[12]O. Benary, L. R. Price, and G. Alexander, Report No. UCRL-20000 NN, 1970 (unpublished).

[13]The total cross section obtained through the optical theorem can be used as a check on the normalization assumption of 31.5 mb as the total elastic cross section. At $T_p = 0.56$ GeV, P. Schwaller *et al.* [CERN Report No. 72-13 (unpublished)] measured σ_T for p-^{4}He scattering as 123.7 ± 1.0 mb. (See Table V.)

[14]S. L. Verbeck, J. C. Fong, G. Igo, C. A. Whitten, Jr., D. L. Hendrie, Y. Terrien, V. Perez-Mendez, and G. W.Hoffmann, Phys. Lett. 59B, 339 (1975); J. Fain, J. Gardes, A. Lefort, L. Meritet, J. F. Panty, G. Peynet, M. Querron, F. Vazeille, and B. Ille, Nucl. Phys. A262, 413 (1976); A. W. Stetz, J. M. Cameron, D. A. Hutcheon, R. H. McCamis, C. A. Miller, G. A. Moss, G. Roy, J. G. Rogers, C. A. Goulding, and W. T. H. VanOers, *ibid.* A290, 285 (1977); J. Berger, J. Duflo, L. Goldzahl, F. Plouin, J. Oostens, M. Van-Den Bossche, L. Vuttai, G. Bizard, C. LeBrun, F. L. Fabbri, P. Picozza and L. Satta.

[15]M. A. Nasser, M. M. Gazzaly, J. V. Geaga, B. Hoistad, G. J. Igo, J. B. McClelland, A. L. Sagle, H. Spinka, J. B. Carroll, V. Perez-Mendez, and E. T. B. Whipple, Nucl. Phys. A (to be published).

[16]J. Berger *et al.*, in *High Energy Physics and Nuclear Structure—1975*, proceedings of the Sixth International Conference, Santa Fe and Los Alamos, edited by D. E. Nagle *et al.* (AIP, New York, 1975).

[17]S. Wallace and Y. Alexander, Phys. Rev. Lett. 38, 1269 (1977).

[18]R. L. Mercer, L. G. Arnold, and B. C.Clark, Phys. Lett. 73B, 9 (1978).

[19]D. V. Bugg, D. C. Salter, G. H. Stafford, R. F. George, K. F. Riley, and R. J. Tapper, Phys. Rev. 146, 980 (1966).

[20]E. T. Boschitz, W. K. Roberts, J. S. Vincent, M. Blecher, K. Gotow, P. C. Gugelot, C. F. Perdrisat, L. W. Swenson, and J. R. Priest, Phys. Rev. C 6, 457 (1972).

[21]J. P. Auger, J. Gillespie, and R. J. Lombard, Nucl. Phys. A212, 372 (1976).

[22]S. Wallace, private communication.

[23]Analyzing power measurements for *pp*, *pn*, and *pd* backward elastic scattering were made at the Argonne ZGS in August, 1977.